Title

Splenic Dendritic Cells Survey Red Blood Cells for Missing Self-CD47 to Trigger Adaptive Immune Responses

Journal

Immunity, 43(4)

ISSN

1074-7613

Authors

Yi, Tangsheng
Li, Jianhua
Chen, Hsin
et al.

Publication Date

2015-10-01

DOI

10.1016/j.immuni.2015.08.021

Peer reviewed

HHS Public Access

Author manuscript

Immunity. Author manuscript; available in PMC 2016 October 20.

Published in final edited form as:

Immunity. 2015 October 20; 43(4): 764–775. doi:10.1016/j.immuni.2015.08.021.

Splenic dendritic cells survey red blood cells for missing self-CD47 to trigger adaptive immune responses

Tangsheng Yi[1,3], **Jianhua Li**[1], **Hsin Chen**[1], **Jiaxi Wu**[1], **Jinping An**[1], **Ying Xu**[1], **Yongmei Hu**[2], **Clifford A. Lowell**[2], and **Jason G. Cyster**[1,4]

[1]Howard Hughes Medical Institute and Department of Microbiology and Immunology, University of California San Francisco, CA 94143, USA

[2]Department of Laboratory Medicine, University of California, San Francisco, CA 94141, USA

Summary

Sheep red blood cells (SRBCs) have long been used as a model antigen for eliciting systemic immune responses yet the basis for their adjuvant activity has been unknown. Here we show that SRBCs failed to engage the inhibitory mouse SIRPα receptor on splenic $CD4^+$ dendritic cells (DCs), and this led to DC activation. Removal of the SIRPα ligand, CD47, from self-RBCs was sufficient to convert them into an adjuvant for adaptive immune responses. DC capture of *Cd47*$^{-/-}$ RBCs and DC activation occurred within minutes in a src-family kinase and CD18 integrin-dependent manner. These findings provide an explanation for the adjuvant mechanism of SRBCs and reveal that splenic DCs survey blood cells for missing self-CD47, a process that may contribute to detecting and mounting immune responses against pathogen-infected RBCs.

Graphical abstract

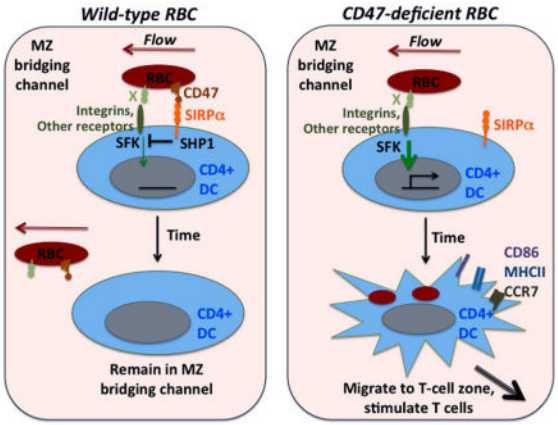

[4]Correspondence should be addressed to: jason.cyster@ucsf.edu.

[3]Current address: Department of Discovery Immunology, Genentech, South San Francisco, CA 94080, USA.

Introduction

The efficacy of xenogeneic red blood cells in promoting antibody responses is instrumental in elucidating key aspects of T cell help of immune responses (Hunter et al., 1974; Jerne and Nordin, 1963; Mitchell and Miller, 1968). In more recent years, SRBCs have been widely used as a simple method to elicit robust $CD4^+$ T cell and antibody responses and to elucidate requirements for germinal center (GC) and memory B cell generation (Dogan et al., 2009; Kraal et al., 1982; Shinall et al., 2000). Clinically, RBC immunogenicity is an important factor in the induction of alloantibody responses against minor histocompatability antigens in 3–6% of people receiving blood-group matched RBC transfusions, and the much higher frequency in Rhesus-antigen mismatched transfusions (Zimring and Hendrickson, 2008). RBC immunogenicity is also likely to be an important factor in the development of autoimmune hemolytic anemia. Since RBCs lack or minimally express major histocompatibility complex (MHC) molecules and are infected by pathogens such as malaria that have had selective influences on the human population, it seems likely that specialized immune-sensing systems have evolved that contribute to RBC immunogenicity. However, despite the long period of study, the molecular basis for foreign RBC adjuvant activity has remained enigmatic.

The mouse spleen contains two major DC subsets, $CD4^+$ and $CD8^+$ DCs, with smaller numbers of double negative DCs (Miller et al., 2012). $CD4^+$ DCs are best defined for their role in promoting $CD4^+$ T cell responses and, in turn, antibody responses, whereas $CD8^+$ DCs have a role in antigen cross-presentation to $CD8^+$ T cells (Miller et al., 2012). $CD4^+$ DCs, particularly those identified by coexpression of the lectin DCIR2, are enriched in regions of the spleen known as marginal zone (MZ)-bridging channels, located between the T zone and red pulp (Witmer and Steinman, 1984). DC positioning in these channels is dependent on the chemoattractant receptor EBI2 (GPR183) (Gatto et al., 2013; Yi and Cyster, 2013). A specialized feature of the spleen is its open circulation, with blood being released in the marginal sinus to then flow through the MZ and on to the red pulp (Mebius and Kraal, 2005). RBCs travel with this flow and after passing through the macrophage rich MZ and red pulp, return to circulation via venous sinuses (Mebius and Kraal, 2005). The positioning of $CD4^+$ DCs in the MZ bridging channel places them in a location that is exposed to RBCs (Yi and Cyster, 2013).

CD47 (also known as integrin associated protein, IAP) is a cell surface protein expressed by most cell types including RBCs (Barclay and Van den Berg, 2014; Oldenborg, 2013). CD47 engagement of the polymorphic signal regulatory protein α (SIRPα) on macrophages transmits a ‘don’t eat me signal’ that prevents cell engulfment. CD47-deficient RBCs, as well as various other cell types such as cancer stem cells, are rapidly cleared from circulation in wild-type mice but not in mice lacking SIRPα (Chao et al., 2012; Oldenborg, 2013). The SIRPα negative signal involves immunoreceptor tyrosine-based inhibitory motif (ITIM)-mediated recruitment of protein tyrosine-phosphatases (SHP1 and SHP2) that counteract pro-phagocytic signals (Barclay and Van den Berg, 2014; Oldenborg, 2013). The pro-phagocytic receptor-ligand systems that trigger phagocytosis of $Cd47^{-/-}$ cells are not well defined but low density lipoprotein (LDL)-related protein-1 (LRP1) on macrophages binding to calreticulin on target cells has been implicated in some situations (Chao et al.,

2010; Gardai et al., 2005). Mice deficient in CD47 or SIRPα have reduced numbers of $CD4^+$ DCs, and this DC-deficiency has been associated with a reduced ability to mount antibody responses (Hagnerud et al., 2006; Saito et al., 2010; Van et al., 2006). However, the basis for the $CD4^+$ DC deficiency in *Cd47*$^{-/-}$ or *Sirp*α$^{-/-}$ mice has not been elucidated.

CD47-SIRPα interactions are not well conserved across species and we report here that sheep RBCs failed to bind mouse SIRPα. We show that SRBCs were strong activators of splenic $CD4^+$ DCs and we go on to show that removal of CD47 from mouse RBCs was sufficient to confer upon them 'SRBC-like' immunogenicity. RBC-mediated splenic $CD4^+$ DC activation occurred extremely rapidly (within minutes) and was then followed after 2–3 days by a DC depletion that phenocopied the splenic DC deficiency in *Cd47*$^{-/-}$ and *Sirp*α $^{-/-}$ mice. *Cd47*$^{-/-}$ RBC-mediated DC activation required signaling via Src-family kinases and was partially dependent on CD18-containing integrins. These data provide an explanation for the adjuvant activity of foreign RBCs and cells with reduced CD47 expression and they reveal a role for splenic MZ-bridging channel DCs in self-RBC surveillance and in triggering immunity against RBCs.

Results

SRBCs activate splenic $CD4^+$ DCs and promote migration to the T zone

During studies on EBI2-mediated MZ bridging-channel positioning of $CD4^+$ DCs we observed that SRBCs could provoke DC CCR7 chemokine receptor upregulation and migration to the T cell zone (Yi and Cyster, 2013). Examining this process in detail, we found that within 6 hours of SRBC injection, splenic $CD4^+$ DCs markedly upregulated CD86 and MHC class II (MHCII) as well as CCR7 (Fig. 1A). This activation effect required intact SRBCs as it did not occur following injection of sonicated cells (Fig. S1A). RNAseq analysis showed that 1 hr following SRBC injection, the DCs increased expression of transcripts for numerous maturation markers, including costimulatory molecules, lysosomal markers, and a range of cytokines and chemokines (Fig. 1B and Table S1). Similar DC activation occurred after transfer of human RBCs (Fig. S1B).

Following injection, many foreign RBCs are captured in the splenic marginal zone by resident macrophages (Hagnerud et al., 2006; Yi and Cyster, 2013). However, ablation of these macrophages by treating *Cd169*-DTR mice with diphtheria toxin (DT) (Miyake et al., 2007) did not prevent DC activation by SRBCs (Fig. S1C). Immunofluorescence microscopy of spleen tissue taken 15 min after PKH26-labelled SRBC injection revealed close association of $CD11c^+$ cells and PKH26-label in MZ bridging channels (Fig. S1D). The DC activation occurred in mice lacking activating Fc receptor expression (*Fcer1g*$^{-/-}$) (Fig. S1E) and in mice treated with cobra venom factor to deplete complement C3 (data not shown) ruling out an essential role for pre-existing (natural) xenoreactive IgG antibodies or the complement factor C3. We next considered whether CD47 might be involved. The CD47 receptor, SIRPα, is highly expressed on splenic $CD4^+$ DCs ((Lahoud et al., 2006) and Fig. S1F, G). SIRPα is polymorphic and known to often bind CD47 in a species-restricted manner (Barclay and Van den Berg, 2014; Oldenborg, 2013; Subramanian et al., 2006). *In vitro* adhesion assays showed that recombinant 129/Sv-derived mouse SIRPα supported adhesion of wild-type (WT) mouse RBCs, but it failed to support adhesion of sheep RBCs

(Fig. 1C) or, as expected (Subramanian et al., 2006), human RBCs (Fig. 1C). Taken together, these data suggest that SRBCs maybe causing $CD4^+$ DC activation due to a failure to adequately engage the negative regulatory SIRPα receptor on the DCs.

CD47-deficient self-RBCs activate splenic $CD4^+$ DCs

We speculated that if a failure to engage the inhibitory SIRPα receptor was the basis for the SRBC adjuvant effect, then removing CD47 from mouse RBCs might be sufficient to make them stimulatory for $CD4^+$ splenic DCs. Consistent with this hypothesis, three hours after injection of *Cd47*$^{-/-}$ RBCs into WT mice, splenic $CD4^+$ DCs became uniformly $CD86^+$, $MHCII^{hi}$ and $CCR7^{hi}$ (Fig. 2A). Injection of *Cd47*$^{-/-}$ RBCs labeled with the red fluorescent membrane dye, PKH26, led to labeling of the majority of splenic $CD4^+$ DCs, indicating they had captured RBC or RBC-derived molecules (Fig. 2A). Two-photon microscopy of vibratome-cut spleens from *Itgax*-YFP^+ mice that had received PKH26-labeled *Cd47*$^{-/-}$ RBCs 20 min before revealed DCs bearing $PKH26^+$ material that were situated in or near MZ bridging channels (Fig. 2B and Movie S1). When splenic $DCIR2^+$ DCs were isolated by flow cytometry 30 min after PKH26-labeled *Cd47*$^{-/-}$ RBC injection and examined by microscopy, many of the DCs were positive for PKH26-label (Fig. 2C).

As little as 5 ul of *Cd47*$^{-/-}$ blood was effective in promoting activation of splenic $CD4^+$ DCs (Fig. S2A). When such low numbers of PKH26-labeled RBCs were injected, only a fraction of the $CD4^+$ DCs became dye labeled. Gating on the $PKH26^{hi}$ versus $PKH26^{lo}$ $CD4^+$ DCs showed that the activation occurred most completely in the cells that had directly captured labeled RBCs or RBC fragments (Fig. 2D), providing evidence that DC activation depended on physical contact with the *Cd47*$^{-/-}$ RBCs. The efficacy of *Cd47*$^{-/-}$ RBCs in causing DC activation was not influenced by the method of RBC preparation as blood isolated in Alsever's solution, EDTA, or heparin had similar DC stimulating activity (Fig. S2B). Injection of white blood cells isolated from 40 ul of *Cd47*$^{-/-}$ blood had no DC stimulatory activity, confirming that the activation was RBC-mediated (Fig. S2C). Time course analysis showed surface CD86 and CCR7 upregulation occurring as early as 1.5 hr after *Cd47*$^{-/-}$ RBC injection and peaking after 6–24 hr (Fig. 2E). $CD8^+$ DCs that express intermediate amounts of SIRPα and are sparse in the MZ showed much less activation and antigen capture (Fig. 2E and Fig. S1F,G & S2D). Immunohistochemical staining of spleen sections showed that *Cd47*$^{-/-}$ RBCs caused $CD4^+$ DCs (identified by their co-expression of DCIR2) to rapidly relocate from the MZ bridging channels in to the T cell zone, favoring the B-T cell zone border region (Fig. 2F).

The above findings established that CD47-deficiency was sufficient to make mouse RBCs stimulatory for mouse DCs. We then asked the reciprocal question: is maintenance of the CD47-SIRPα interaction sufficient to prevent xenogeneic RBCs from causing DC activation? Previous work has shown that while human CD47 does not bind well to most strains of mouse SIRPα, it does bind strongly to the variant of SIRPα expressed in the non-obese diabetic (NOD) strain (Kwong et al., 2014; Takenaka et al., 2007). When human RBCs were transferred to NOD mice, DC activation did not occur whereas it was readily observed when the mice received *Cd47*$^{-/-}$ mouse RBCs (Fig. 2G). These findings further

support the conclusion that lack of CD47- SIRPα engagement is the main mechanism for xenogeneic RBC-mediated activation of splenic DCs.

Splenic CD4$^+$ DC-deficiency in *Cd47*$^{-/-}$ mice due to chronic signaling

If DC activation were occurring solely as a consequence of CD47-deficiency on RBCs then we speculated that short-term treatment with a SIRPα antagonistic antibody should similarly lead to CD4$^+$ DC activation. Consistent with this model, six hours after injection of a SIRPα function-blocking antibody (Oldenborg 2000 Science; Oldenborg 2001 JEM; Wang, 2007 Blood), CD4$^+$ DCs and to a much lesser extent CD8$^+$ DCs, showed upregulation of CD86, MHCII and CCR7 (Fig. 3A and S3A) and CD4$^+$ DCs relocated from MZ bridging channels into the T cell zone (Fig. 3B). Previous work has shown that SIRPα- and CD47-deficient mice have a selective deficiency in splenic CD4$^+$ DCs ((Hagnerud et al., 2006; Saito et al., 2010; Van et al., 2006) and Fig. S3B, C), but the basis for this deficiency has been unclear. We speculated that it might be a consequence of constant maturation-inducing signaling occurring in DCs due to the lack of an RBC CD47-triggered negative regulatory signal. Maturation-inducing signals of other types are known to shorten DC lifespan (De Trez et al., 2005). Flow cytometric analysis of the DCs remaining in *Cd47*$^{-/-}$ mice showed that the CD4$^+$ but not CD8$^+$ DCs had reduced SIRPα surface abundance, suggesting that the inhibitory receptor may be internalized in the absence of ongoing engagement with CD47 (Fig. 3C). Importantly, when WT mice were injected with *Cd47*$^{-/-}$ RBCs, following the initial period of DC activation, the CD4$^+$ DCs became depleted as assessed both by flow cytometry (Fig. 3D, left panel) and immunohistochemistry for DCIR2 (Fig. 2E). A similar CD4$^+$ DC depletion occurred three days after anti-SIRPα injection (Fig. 3D, right panel). If CD4$^+$ DCs in *Cd47*$^{-/-}$ mice were continually being matured and depleted by endogenous RBCs, it seemed likely that they would be hypo-responsive to further stimulation by this pathway. A prior report found that *Cd47*$^{-/-}$ mice mounted poor antibody responses against SRBCs though the defect was attributed to the reduction in DC number (Hagnerud et al., 2006). We found that the CD4$^+$ DCs remaining in *Cd47*$^{-/-}$ mice were not activated by SRBCs whereas they were fully responsive to LPS (Fig. 3F).

Cd47$^{-/-}$ self-RBCs have potent adjuvant activity

To test whether *Cd47*$^{-/-}$ mouse RBCs could function as an adjuvant for CD4$^+$ T cell responses, ovalbumin (OVA) was coupled to *Cd47*$^{-/-}$ or WT RBCs and injected into mice harboring OVA-specific OTII CD4$^+$ T cells. Marked proliferation of the OTII CD4$^+$ T cells occurred in the recipients of *Cd47*$^{-/-}$, but not WT OVA-RBCs (Fig. 4A). A similar experiment with OVA-specific OTI CD8$^+$ T cells showed a lesser but still significant difference between mice receiving *Cd47*$^{-/-}$ and WT OVA-RBCs (Fig. 4A). Phenotypic analysis of the responding CD4$^+$ OTII T cells at day three showed they upregulated ICOS, PD1, and CXCR5, markers of follicular helper T cells (Fig. 4B and S4D). When mice were immunized with OVA-coupled DCIR2 antibody, *Cd47*$^{-/-}$ RBCs again had an adjuvant effect indicating that their action was through DC activation and not solely through promoting capture of RBC-bound antigen (Fig. S4A). No OTII T cell proliferation was observed in mice treated with *Cd47*$^{-/-}$ RBCs in the absence of OVA (Fig. S4B). In another approach we tested whether the DC activation occurring after SIRPα blockade (Fig. 2) was

sufficient to augment T cell responses. In mice immunized with OVA-coupled DCIR2 antibody, SIRPα blockade led to increased proliferation of OVA-specific T cells (Fig. S4C).

We speculated that, if the adjuvant activity of SRBCs occurs by DCs binding these xenogeneic cells but failing to receive a SIRPα-negative signal, then this pathway should be disrupted in *Cd47*$^{-/-}$ hosts due to SIRPα already being fully disengaged and unable to distinguish SRBCs from endogenous RBCs. Consistent with this interpretation, OTII T cells showed 80 percent lower expansion in *Cd47*$^{-/-}$ hosts than in WT hosts in response to OVA-SRBCs (Fig. 4C) and less induction of PD1 and ICOS (Fig. S4D). In accord with this defect, the *Cd47*$^{-/-}$ hosts failed to mount a GC response to SRBCs, as examined by flow cytometry (Fig. 4D) and immunohistochemistry using the GL7 GC marker (Fig. 4E). *Ebi2*$^{-/-}$ mice have a similar deficiency in CD4^{+} DC numbers as *Cd47*$^{-/-}$ mice (Gatto et al., 2013; Yi and Cyster, 2013), but they are expected to have intact SIRPα function and they had normal DC SIRPα expression (Fig. S4F); these mice mounted a GC response of normal magnitude following SRBC immunization (Fig. 4F). Moreover, the *Cd47*$^{-/-}$ mice mounted a normal splenic GC response to viral-like particles (VLPs) that contain toll-like receptor (TLR)-stimulating nucleic acids (Fig. 4F). These observations support the conclusion that SRBCs activate the mouse immune system by failing to engage SIRPα on DCs.

Self-RBCs activate CD4^{+} DCs via Src-family kinase signaling

Cd47$^{-/-}$ mouse RBCs were effective in promoting CD4^{+} DC activation in mice lacking Myd88 and Trif, thus excluding a requirement for TLR receptors in RBC-triggered DC activation (Fig. 5A). Since SIRPα is generally thought to inhibit signaling by recruiting protein tyrosine phosphatases (particularly SHP1 in myeloid cells) (Oldenborg, 2013; Oldenborg et al., 2001) we tested whether Src family tyrosine kinases (SFKs) were required for *Cd47*$^{-/-}$ RBC-mediated DC activation. Analysis of mice lacking individual SFKs Hck, Fgr, or Lyn known to be important in neutrophil and macrophage signaling (Abram and Lowell, 2009) showed little effect on the DC response (Fig. S5A), but when Hck, Fgr and Lyn were all removed, DC activation and repositioning in response to *Cd47*$^{-/-}$ RBCs was blocked (Fig. 5B, C) while activation by LPS remained intact (fig. S5B). Hck, Fgr and Lyn triple-deficient mice had normal or increased numbers of CD4^{+} DCs and they were positioned comparably to wild-type cells (Fig. 5C and S5C). Similar DC activation defects were observed in mixed bone marrow (BM) chimeras establishing that the SFK requirement was DC intrinsic (Fig. 5D and Fig. S5D). As a further test of the DC SFK requirement, we generated 50:50 mixed SFK-deficient:*Zbtb4*6-DTR BM chimeras and treated them with DT to ablate the wild-type DCs and leave only SFK-deficient DCs. *Cd47*$^{-/-}$ RBCs again failed to activate the SFK-deficient DCs (Fig. S5E). Syk often functions downstream of SFKs (Lowell, 2011) and consistent with this kinase contributing to DC activation, CCR7 was less completely induced in CD4^{+} DCs in *Syk*$^{-/-}$ fetal liver chimeras that had been injected with *Cd47*$^{-/-}$ RBCs or SRBCs (Fig. S5F). Analysis of downstream signaling revealed rapid *in vivo* upregulation of phospho-p38, pS6, pERK and pCREB in a SFK-dependent manner in CD4^{+} DCs following *Cd47*$^{-/-}$ RBC injection (Fig. 5E and F). Phospho-p38 and pERK had already peaked 5 min after RBC injection whereas pCREB reached a maximum at 60 min (Fig. 5E).

CD18-containing integrins are involved in RBC-mediated DC activation

DC express a wide range of receptors capable of activating SFKs though whether any of these molecules bind RBCs is not known (Sancho and Reis e Sousa, 2012). Many C-type lectin receptors depend on the ITAM-containing adaptors DAP12 or Fcεr1γ for surface expression and signaling (Lowell, 2011; Sancho and Reis e Sousa, 2012). Analysis of mice double-deficient for DAP12 (*Tyrobp*$^{-/-}$) and FcεRIγ showed that *Cd47*$^{-/-}$ RBCs induced DC activation normally (Fig. 6A). Some receptors signal through another partner known as DAP10 (Lanier, 2009), but mice lacking the *Hcst* gene that encodes this co-receptor also activated normally in response to *Cd47*$^{-/-}$ RBCs (not shown). Another important group of SFK-activating receptors are the integrins (Lowell, 2011). The CD18 (Itgβ2)-containing integrins CD11b and CD11c are defining markers of CD4^{+} DCs (Steinman et al., 1997) and these cells also express high amounts of CD11a (LFA1) (Balkow et al., 2010). We found that *Cd47*$^{-/-}$ RBCs were inefficiently captured by DCIR2^{+} CD4^{+} DCs in *Itgb2*$^{-/-}$ mice and the integrin-deficient DCs showed minimal activation (Fig. 6B). The spleens of *Itgb2*$^{-/-}$ mice are enlarged due to myeloid hyperplasia in the red pulp (Scharffetter-Kochanek et al., 1998), making it possible that the requirement for CD18 was indirect. To test for an intrinsic integrin requirement, we established *Itgb2*$^{-/-}$:WT mixed BM chimeras. In these animals the CD18-deficient cells were selectively compromised in capturing and becoming activated by *Cd47*$^{-/-}$ RBCs, (Fig. 6C, D). As a further method to test the intrinsic role of CD18 in DCs we generated mixed *Itgb2*$^{-/-}$*:Zbtb46*-DTR chimeras and treated the animals with DT to selectively ablate wild-type DCs prior to RBC injection. CD18-deficient DCs again showed reduced capture of *Cd47*$^{-/-}$ RBCs and less induction of CCR7 (Fig. S6A). Tissue sections from these mice revealed that CD18-deficient and wild-type DCs were distributed similarly in control chimeras that received wild-type RBCs (Fig. S6B) and there was incomplete relocalization of *Itgb2*$^{-/-}$ DCs to the outer T cell zone 6 hours after *Cd47*$^{-/-}$ RBC injection (Fig. S6B). These findings provide evidence that CD18-containing integrins function intrinsically in DCs during activation by CD47-deficient RBCs. However, some PKH26 acquisition and DC activation was still observable in each of these conditions, indicating that there are additional mechanisms of DC-RBC engagement and DC activation.

Although LRP1 has been implicated in macrophage uptake of *Cd47*$^{-/-}$ apoptotic cells and RBCs by binding surface exposed calreticulin (Gardai et al., 2005; Nilsson et al., 2012), *Lrp1*$^{-/-}$ DCs responded normally to *Cd47*$^{-/-}$ RBCs (Fig. S6C). Finally, we tested the impact of CD18-integrin deficiency on the ability to mount CD4 T cell responses. When *Itgb2*$^{-/-}$ BM chimeras were immunized with OVA-conjugated *Cd47*$^{-/-}$ RBCs they mounted a diminished wild-type OTII T cell proliferative response compared to the response in control BM chimeras (Fig. S6D). Taken together, these findings provide evidence that CD18-containing integrins contribute to the efficiency of DC activation by *Cd47*$^{-/-}$ self-RBCs.

Discussion

CD47 is a marker of ‘self’ on RBCs and cells lacking CD47 are rapidly cleared from the bloodstream by macrophages (Oldenborg et al., 2000). Our findings provide evidence that splenic bridging channel DCs survey RBCs for missing self-CD47. When CD47 is absent or of a type unable to engage mouse SIRPα, CD4^{+} DCs are rapidly alerted and become

competent to stimulate CD4 T cell and antibody responses. The concept of immune cell activation by missing self recognition is best established for NK cell activation by cells with reduced or absent MHC class I (Lanier, 2005; Medzhitov and Janeway, 2002). NK cells utilize a family of ITIM-containing receptors that recognize self-MHC class I to inhibit signaling via activating receptors. Loss of CD47 from RBCs may act to alert DCs that RBCs are in an altered state in a similar way to how loss of MHC class I alerts NK cells that nucleated cells are in an altered state.. MHC class I is downregulated during many types of viral infection and also on many cancer cells. We speculate that RBC CD47 becomes reduced or less accessible to SIRPα following infection by certain RBC-tropic pathogens, leading to DC activation and immunity.

The inhibitory 'don't eat me' signal transmitted by SIRPα engagement in macrophages has been well characterized (Barclay and Van den Berg, 2014; Chao et al., 2012; Oldenborg, 2013), but the positive signal that it counteracts has been less clear. We identify signaling via SFKs as an important positive signal in DCs. Our data support a model where, in the healthy state, RBC CD47 engagement of bridging channel DC SIRPα transmits negative signals that over-ride positive SFK-signals from surface receptors, the RBC travels on to the red pulp and the DC remains in a quiescent state. However, when CD47 surface amounts or availability are reduced, the positive SFK signals dominate over SIRPα negative signals, leading to RBC uptake and DC activation and movement to the T cell zone to promote cognate T cell and antibody responses. The uptake step, whether of intact RBC or RBC fragments, is likely to involve tyrosine phosphorylation of several cytoskeletal proteins as observed during *in vitro* studies of IgG-opsonized SRBC phagocytosis by human macrophages (Tsai and Discher, 2008).

The factors influencing CD47 abundance on RBCs are not fully understood but the amounts reduce gradually on aging of the cells (Oldenborg, 2013) and after periods of *in vitro* storage (Gilson et al., 2009; Stewart et al., 2005). CD47 in human RBCs exists in the membrane as a multiprotein complex (Oldenborg, 2013). Loss of some members of this complex, such as the Rh antigen or band 3 leads to reduced CD47 expression (Oldenborg, 2013). The membrane mobility and clustering of CD47 is also affected when components of the complex are missing (Oldenborg, 2013) and when membrane lipid composition changes (Lv et al., 2015). We found in the mouse that $Cd47^{+/-}$ RBCs failed to stimulate DCs in wild-type recipients (unpubl. obs.) indicating that CD47 surface density may need to fall more than 50% to cause DC activation. However, CD47 in mouse RBCs is not in the same type of complex as in human RBCs making direct comparisons of mouse and human RBCs difficult (Oldenborg, 2013). In future studies it maybe possible to take advantage of our finding that NOD SIRPα interacts with human CD47 adequately to inhibit DC activation to test whether treatments, mutations or infections that affect human CD47 abundance or distribution in the membrane diminish SIRPα engagement to an extent that leads to DC activation. Such studies may help discern whether this DC activation pathway contributes to the high frequency of autoimmune hemolytic anemia in Rh^- individuals (Oldenborg, 2013) and the immunogenicity of stored allo-RBCs (Gilson et al., 2009; Hendrickson et al., 2010).

We suggest that positioning in MZ bridging channels allows $CD4^+$ DCs to survey a large number of passing self-RBCs for altered or missing self-CD47 expression. White blood cells

(WBCs) are also likely being surveyed in the same way, but given that RBCs out number WBCs by about 1000 to 1, a major purpose of DC positioning in the bridging channels may be for exposure to the non-migratory RBCs. RBC engagement of DCs is likely to be occurring under fluid shear stress, providing forces that promote integrin-mediated adhesion and signaling (Woolf et al., 2007). Although RBCs express little if any of the CD18 integrin ligands ICAM1 or ICAM2, human and mouse RBCs express ICAM4 (Bailly et al., 1994; Bailly et al., 1995; Lee et al., 2006; Lee et al., 2003). *In vitro* studies have shown that human ICAM4 can bind all three CD18-containing integrins (Cartron and Elion, 2008; Ihanus et al., 2007; Lee et al., 2003). However, using previously established *Icam4*$^{-/-}$ mice (Lee et al., 2006), we found that *Icam4*$^{-/-}$ *Cd47*$^{-/-}$ RBCs were captured by and activated DCs equivalently to *Icam4*$^{+/+}$ *Cd47*$^{-/-}$ cells (unpubl. obs.) suggesting that RBC display additional ligands for CD18-containing integrins. Alternatively, it is possible that CD18-containing integrins are acting in an indirect way to augment DC access to RBCs. Although we did not observe major alterations in DC positioning in the spleens of DT-treated *Itgb2*$^{-/-}$ versus wild-type *Zbtb46*-DTR mixed BM chimeras, we cannot exclude the possibility that there are local cell-positioning or cell-cell interaction differences that affect the extent of exposure to rapidly moving blood cells. Additionally, since we did detect measurable binding of *Cd47*$^{-/-}$ RBCs to *Itgb2*$^{-/-}$ DCs, there are likely to be further SFK-activating receptors on CD4^{+} DCs that have ligands on RBCs. Pro-phagocytic signaling during CD47-deficient cell binding by macrophages involves LRP1 engagement of surface exposed calreticulin on target cells (Chao et al., 2010; Gardai et al., 2005). CD4^{+} DCs express only low amounts of LRP1 (Subramanian et al., 2014) and this receptor did not contribute to DC activation by RBCs. However, it remains plausible that other calreticulin receptors exist on DCs and these could work together with integrins to promote DC activation.

Uptake of cancer cells by macrophages following CD47 blockade leads to antigen presentation and stimulation of CD8^{+} but not CD4^{+} T cell responses (Tseng et al., 2013). In that work, CD47-blocked target cells failed to activate DCs *in vitro* to a state with CD4^{+} T cell stimulatory properties (Tseng et al., 2013). Consistent with those observations, we were unable to observe activation of splenic DCs *in vitro* by SRBCs or *Cd47*$^{-/-}$ RBCs (unpubl. obs.). This may be a consequence of the background extent of DC maturation that occurs when splenic DCs are isolated and incubated *in vitro*, but may also reflect a need for features of the *in vivo* environment, such as exposure to shear forces, that are not mimicked in the culture system. However, *in vitro* studies of human blood-derived DCs have revealed an ability of SIRPα engagement by CD47-Fc or RBCs to diminish DC activation (Latour et al., 2001; Schakel et al., 2006). The basis for this discrepancy between mouse and human *in vitro* studies is unclear, but these data do suggest that our *in vivo* observations will translate to humans.

The basis for the CD4^{+} DC-deficiency in CD47- and SIRPα-deficient mice has been unclear (Hagnerud et al., 2006; Saito et al., 2010; Van et al., 2006), though one study provided evidence that engagement of DC SIRPα by CD47 on both hematopoietic and stromal cells is involved (Saito et al., 2010). By showing that blockade of SIRPα or transient treatment with *Cd47*$^{-/-}$ RBCs is sufficient to cause a similar deficiency of splenic CD4^{+} DCs after 3 days as full CD47- or SIRPα-deficiency, we provide support for a model where unrestrained

RBC-mediated transmission of activation signals causes sustained DC depletion. This model is consistent with the observation that SIRPα-deficient $CD4^+$ DCs turnover at an accelerated rate (Saito et al., 2010). We speculate that RBC-triggered maturation of DCs is followed by their loss due to apoptosis as has been observed following splenic DC exposure to LPS (De Trez et al., 2005). We do not exclude that CD47 on additional cell types contributes to maintaining DC quiescence (Saito et al., 2010; Wang et al., 2007). (Saito et al., 2010)CD47 and SIRPα-deficient mice have DC reductions in lymph nodes (LNs), epidermis and lamina propria as well as spleen (Saito et al., 2010; Scott et al., 2014; Washio et al., 2015). Given that DCs in non-splenic locations may not be regularly exposed to RBCs, these deficiencies might indicate that DC interactions with other $CD47^+$ cell types are important, but it is also possible that other functions of SIRPα and CD47 are needed in different DC types (Barclay and Van den Berg, 2014).

Finally, our demonstration that CD47-deficient RBCs can serve as adjuvants for $CD4^+$ T cell and antibody responses adds to recent literature highlighting CD47 antagonism as an approach to augment macrophage responses against cancer cells and parasite infected RBCs (Banerjee et al., 2015; Chao et al., 2012; Tseng et al., 2013). Induction of $CD4^+$ T cell and antibody responses during CD47-blockade treatments might contribute to the anti-tumor and anti-pathogen effects. Such approaches may also be valuable in the design of vaccines for promoting immune responses against malaria and other RBC-tropic pathogens.

Experimental procedures

Mice

C57BL/6NCr and C57BL/6-cBrd/cBrd/Cr (CD45.1) mice at age 7–9 weeks were purchased from National Cancer Institute (Frederick, MD). NOD mice were from an internal UCSF colony and were provided by Qizhi Tang. OVA-specific OTII or OTI TCR-transgenic mice and $Cd47^{-/-}$ and $Cd18^{-/-}$ mice were purchased from Jackson laboratory (Bar Harbor, ME). $Ebi2^{-/-}$, $Lyn^{-/-}$, $Fgr^{-/-}$, $Hck^{-/-}$ $Myd88^{-/-}Trif^{-/-}$, $Fcer1g^{-/-}$, $Fcer1g^{-/-}Tyrobp^{-/-}$, $Hcst^{-/-}$, $Lyn^{-/-}Fgr^{-/-}Hck^{-/-}$, and $Syk^{-/-}$ mice were previously established (Bakker et al., 2000; Lowell et al., 1994; Meng and Lowell, 1997; Pereira et al., 2009; Takai et al., 1994; Turner et al., 1995; Yamamoto et al., 2003) and have been backcrossed onto the C57BL/6 background for at least 10 generations. CD169DTR mice (Miyake et al., 2007) were kindly provided by Masato Tanaka (RIKEN Research Center for Allergy and Immunology, Yokohama, Kanagawa, Japan). Zbtb46-DTR mice (Meredith et al., 2012) were from Jackson Laboratory. BM from $Lrp1^{flox/flox}$ $CD11c^{cre/+}$ mice (Subramanian et al., 2014) was provided by Ira Tabas (Columbia Univ., New York, NY). For bone marrow (BM) or fetal liver chimeras, mice were lethally irradiated by exposure to 1300 rads of γirradiation in two doses 3hr apart and BM cells or fetal liver cells ($2\sim5x10^6$) were transferred through the tail vein. Chimeric mice were in most cases analyzed 6–10 weeks after reconstitution. Diphtheria toxin (DT) (EMD Biosciences) was i.p. injected in 1μg doses at days −4 and −1 or as indicated and the mice received RBCs at day 0. Animals were housed in a specific pathogen-free environment in the Laboratory Animal Research Center at the University of California, San Francisco, and all experiments conformed to ethical principles and guidelines approved by the Institutional Animal Care and Use Committee.

Virus-like particles and LPS immunization

Generation and packaging of virus-like particles (VLPs) containing bacteriophage Qβ antigens and CpG ODN G10 were described in detail previously (Jegerlehner et al., 2007). For mouse immunization and induction of GCs, mice were injected intraperitoneally with 50 μg VLPs-CpG. LPS (TLR grade) was obtained from Axxora (Farmingdale, NY) and mice were intravenously injected with 20μg LPS.

Immunohistochemical staining and two-photon imaging

Cryosections of 7 μm were fixed and stained immunohistochemically as previously described (Allen et al., 2004) with the following antibodies: PE-conjugated anti-IgD (11–26c.2a; Biolegend), biotin-conjugated anti-GL7 (GL7, Biolegend), and FITC-conjugated 33D1 antibody (33D1, Biolegend). Images were captured with a Zeiss AxioOberver Z1 inverted microscope. For multiphoton imaging, CD11cYFP mice were injected with PKH26 (Sigma-Aldrich)-labeled *Cd47*$^{-/-}$ RBCs 20 mins before the spleen was harvested and sectioned longitudinally with a vibratome (Leica). The cut spleen was perfused with RPMI1640 medium (Life Technologies) plus 10mM HEPES and 95% CO_2 5% O_2. The cut spleen was imaged with a 7MP two-photon microscope (Carl Zeiss) equipped with a Chameleon laser (Coherent). Excitation wavelengths were 940nm for YFP and 800nm for PKH26. The z-stack was 21μm thick with 3μm intervals. The image was acquired with ZEN2012 (Carl Zeiss) and the three dimensional movie was made with Imaris 7.4.2 x64 (Bitplane).

CD47-Sirpa adhesion assay

A modified version of a previously reported assay was used (Subramanian et al., 2006). Briefly, recombinant 129/Sv strain mouse Sirpα-Fc chimera protein (sequence ID P97797, R&D system, Minneapolis, MN) was coated on high binding ELISA plates in serial dilutions. 129/Sv SIRPα is 96% identical to C57Bl/6 SIRPα and the proteins have similar CD47 binding characteristics (Kwong et al., 2014; Takenaka et al., 2007). After overnight incubation at 4°C, plates were washed wit h PBS and blocked with HBSS buffer containing 1% fatty acid-free BSA at 37°C fo r 2hrs. After blockade, plates were washed twice, added with 50μl RBCs ($1x10^5$/μl) diluted in HBSS with 1% BSA, and then incubated in a 37°C cell incubator for 1hr. After incubation, non-adhered cells were washed away gently with PBS for 6 times. Subsequently, 50μl water was added to the wells for 30min to completely lyse the adhered cells. RBCs have pseudoperoxidase activity of hemoglobin and the relative numbers of RBCs were quantified by adding TMB peroxidase (HRP) substrate (Vector laboratories; Burlingame, CA) to RBC-water solution for 2–5mins. 25μl stop solution (2M Sulfuric acid) was then used to stop the reaction and the plate was read at 450nM with 540nm as the correction wavelength. The dosage curve was calculated with 4-parameter curve fit. An additional experiment was performed using a biotinylated fusion protein of C57BL/6 Sirpα domain-1 and rat CD4 domains 3 and 4 (Kwong et al., 2014) and this behaved similarly to the 129/Sv strain Sirpα-Fc in showing minimal binding of SRBC while supporting strong binding of wild-type mouse RBC.

RNA-seq analysis

Flow cytometric sorted DCs ($1.0x10e^6$) were snap frozen in liquid nitrogen and stored at -80°C and RNA was extracted using the Qiagen RNeasy Kit. RNA quality was checked using the Agilent 2100 Bioanalyzer (RIN > 9 for all samples). Barcoded sequencing libraries were then generated using 100ng of RNA with the Ovation RNA-seq System V2 and Encore Rapid Library System. The UCSF Human Genetics Core performed next-generation sequencing (Illumina HiSeq 2500) with 100bp paired end reads. Sequences were reported as FASTQ files, which were aligned to the mm9 mouse genome using STAR (Spliced Transcript Alignment to a Reference). Generation of Log2FC values and further analyses were performed using a Bioconductor package on RStudio. Data have been deposited in GEO under accession number 71165.

Supplementary Material

Refer to Web version on PubMed Central for supplementary material.

Acknowledgments

We thank Gregory Barton and Lewis Lanier for mice, Martin Bachmann for virus-like particles, Carl Gahmberg for 1A1 anti-ICAM4 antibody, Manikandan Subramanian, Ira Tabas and Joachim Herz for *Lrp1*$^{fl/fl}$ *Itgax*-Cre^{+} bone marrow, Neil Barclay, Lai Shan Kwong, and Chris Garcia for the B6 Sirpαreagents, and Robert Horton and Erick Lu for help with RNAseq analysis and data deposition. Tangsheng Yi was a recipient of Irvington postdoctoral fellowship from the Cancer Research Institute. J.G.C. is an Investigator of the Howard Hughes Medical Institute. The work was supported in part by a grant from the National Institutes of Health (AI40098).

References

Abram CL, Lowell CA. The ins and outs of leukocyte integrin signaling. Annu Rev Immunol. 2009; 27:339–362. [PubMed: 19302044]

Allen CD, Ansel KM, Low C, Lesley R, Tamamura H, Fujii N, Cyster JG. Germinal center dark and light zone organization is mediated by CXCR4 and CXCR5. Nat Immunol. 2004; 5:943–952. [PubMed: 15300245]

Bailly P, Hermand P, Callebaut I, Sonneborn HH, Khamlichi S, Mornon JP, Cartron JP. The LW blood group glycoprotein is homologous to intercellular adhesion molecules. Proc Natl Acad Sci U S A. 1994; 91:5306–5310. [PubMed: 8202485]

Bailly P, Tontti E, Hermand P, Cartron JP, Gahmberg CG. The red cell LW blood group protein is an intercellular adhesion molecule which binds to CD11/CD18 leukocyte integrins. Eur J Immunol. 1995; 25:3316–3320. [PubMed: 8566017]

Bakker AB, Hoek RM, Cerwenka A, Blom B, Lucian L, McNeil T, Murray R, Phillips LH, Sedgwick JD, Lanier LL. DAP12-deficient mice fail to develop autoimmunity due to impaired antigen priming. Immunity. 2000; 13:345–353. [PubMed: 11021532]

Balkow S, Heinz S, Schmidbauer P, Kolanus W, Holzmann B, Grabbe S, Laschinger M. LFA-1 activity state on dendritic cells regulates contact duration with T cells and promotes T-cell priming. Blood. 2010; 116:1885–1894. [PubMed: 20530790]

Banerjee R, Khandelwal S, Kozakai Y, Sahu B, Kumar S. CD47 regulates the phagocytic clearance and replication of the Plasmodium yoelii malaria parasite. Proc Natl Acad Sci U S A. 2015; 112:3062–3067. [PubMed: 25713361]

Barclay AN, Van den Berg TK. The interaction between signal regulatory protein alpha (SIRPalpha) and CD47: structure, function, and therapeutic target. Annu Rev Immunol. 2014; 32:25–50. [PubMed: 24215318]

Cartron JP, Elion J. Erythroid adhesion molecules in sickle cell disease: effect of hydroxyurea. Transfus Clin Biol. 2008; 15:39–50. [PubMed: 18515167]

Chao MP, Jaiswal S, Weissman-Tsukamoto R, Alizadeh AA, Gentles AJ, Volkmer J, Weiskopf K, Willingham SB, Raveh T, Park CY, et al. Calreticulin is the dominant pro-phagocytic signal on multiple human cancers and is counterbalanced by CD47. Sci Transl Med. 2010; 2:63ra94.

Chao MP, Weissman IL, Majeti R. The CD47-SIRPalpha pathway in cancer immune evasion and potential therapeutic implications. Curr Opin Immunol. 2012; 24:225–232. [PubMed: 22310103]

De Trez C, Pajak B, Brait M, Glaichenhaus N, Urbain J, Moser M, Lauvau G, Muraille E. TLR4 and Toll-IL-1 receptor domain-containing adapter-inducing IFN-beta, but not MyD88, regulate Escherichia coli-induced dendritic cell maturation and apoptosis in vivo. Journal of immunology. 2005; 175:839–846.

Dogan I, Bertocci B, Vilmont V, Delbos F, Megret J, Storck S, Reynaud CA, Weill JC. Multiple layers of B cell memory with different effector functions. Nat Immunol. 2009; 10:1292–1299. [PubMed: 19855380]

Gardai SJ, McPhillips KA, Frasch SC, Janssen WJ, Starefeldt A, Murphy-Ullrich JE, Bratton DL, Oldenborg PA, Michalak M, Henson PM. Cell-surface calreticulin initiates clearance of viable or apoptotic cells through trans-activation of LRP on the phagocyte. Cell. 2005; 123:321–334. [PubMed: 16239148]

Gatto D, Wood K, Caminschi I, Murphy-Durland D, Schofield P, Christ D, Karupiah G, Brink R. The chemotactic receptor EBI2 regulates the homeostasis, localization and immunological function of splenic dendritic cells. Nature Immunology. 2013

Gilson CR, Kraus TS, Hod EA, Hendrickson JE, Spitalnik SL, Hillyer CD, Shaz BH, Zimring JC. A novel mouse model of red blood cell storage and posttransfusion in vivo survival. Transfusion. 2009; 49:1546–1553. [PubMed: 19573176]

Hagnerud S, Manna PP, Cella M, Stenberg A, Frazier WA, Colonna M, Oldenborg PA. Deficit of CD47 results in a defect of marginal zone dendritic cells, blunted immune response to particulate antigen and impairment of skin dendritic cell migration. Journal of immunology. 2006; 176:5772–5778.

Hendrickson JE, Hod EA, Spitalnik SL, Hillyer CD, Zimring JC. Storage of murine red blood cells enhances alloantibody responses to an erythroid-specific model antigen. Transfusion. 2010; 50:642–648. [PubMed: 19906034]

Hunter PM, Kappler JW, Kettman JR. The frequency and activity of single helper T cells. Journal of immunology. 1974; 113:830–834.

Ihanus E, Uotila LM, Toivanen A, Varis M, Gahmberg CG. Red-cell ICAM-4 is a ligand for the monocyte/macrophage integrin CD11c/CD18: characterization of the binding sites on ICAM–4. Blood. 2007; 109:802–810. [PubMed: 16985175]

Jegerlehner A, Maurer P, Bessa J, Hinton HJ, Kopf M, Bachmann MF. TLR9 signaling in B cells determines class switch recombination to IgG2a. Journal of immunology. 2007; 178:2415–2420.

Jerne NK, Nordin AA. Plaque Formation in Agar by Single Antibody-Producing Cells. Science. 1963; 140:405.

Kraal G, Weissman IL, Butcher EC. Germinal centre B cells: antigen specificity and changes in heavy chain class expression. Nature. 1982; 298:377–379. [PubMed: 6806671]

Kwong LS, Brown MH, Barclay AN, Hatherley D. Signal-regulatory protein alpha from the NOD mouse binds human CD47 with an exceptionally high affinity-- implications for engraftment of human cells. Immunology. 2014; 143:61–67. [PubMed: 24786312]

Lahoud MH, Proietto AI, Gartlan KH, Kitsoulis S, Curtis J, Wettenhall J, Sofi M, Daunt C, O'Keeffe M, Caminschi I, et al. Signal regulatory protein molecules are differentially expressed by CD8-dendritic cells. Journal of immunology. 2006; 177:372–382.

Lanier LL. NK cell recognition. Annu Rev Immunol. 2005; 23:225–274. [PubMed: 15771571]

Lanier LL. DAP10- and DAP12-associated receptors in innate immunity. Immunol Rev. 2009; 227:150–160. [PubMed: 19120482]

Latour S, Tanaka H, Demeure C, Mateo V, Rubio M, Brown EJ, Maliszewski C, Lindberg FP, Oldenborg A, Ullrich A, et al. Bidirectional negative regulation of human T and dendritic cells by CD47 and its cognate receptor signal-regulator protein-alpha: down-regulation of IL-12 responsiveness and inhibition of dendritic cell activation. Journal of immunology. 2001; 167:2547–2554.

Lee G, Lo A, Short SA, Mankelow TJ, Spring F, Parsons SF, Yazdanbakhsh K, Mohandas N, Anstee DJ, Chasis JA. Targeted gene deletion demonstrates that the cell adhesion molecule ICAM-4 is critical for erythroblastic island formation. Blood. 2006; 108:2064–2071. [PubMed: 16690966]

Lee G, Spring FA, Parsons SF, Mankelow TJ, Peters LL, Koury MJ, Mohandas N, Anstee DJ, Chasis JA. Novel secreted isoform of adhesion molecule ICAM-4: potential regulator of membrane-associated ICAM-4 interactions. Blood. 2003; 101:1790–1797. [PubMed: 12406883]

Lowell CA. Src-family and Syk kinases in activating and inhibitory pathways in innate immune cells: signaling cross talk. Cold Spring Harb Perspect Biol. 2011; 3:a002352. [PubMed: 21068150]

Lowell CA, Soriano P, Varmus HE. Functional overlap in the src gene family: inactivation of hck and fgr impairs natural immunity. Genes & development. 1994; 8:387–398. [PubMed: 8125254]

Lv Z, Bian Z, Shi L, Niu S, Ha B, Tremblay A, Li L, Zhang X, Paluszynski J, Liu M, et al. Loss of Cell Surface CD47 Clustering Formation and Binding Avidity to SIRPalpha Facilitate Apoptotic Cell Clearance by Macrophages. Journal of immunology. 2015

Mebius RE, Kraal G. Structure and function of the spleen. Nat Rev Immunol. 2005; 5:606–616. [PubMed: 16056254]

Medzhitov R, Janeway CA Jr. Decoding the patterns of self and nonself by the innate immune system. Science. 2002; 296:298–300. [PubMed: 11951031]

Meng F, Lowell CA. Lipopolysaccharide (LPS)-induced macrophage activation and signal transduction in the absence of Src-family kinases Hck, Fgr, and Lyn. The Journal of experimental medicine. 1997; 185:1661–1670. [PubMed: 9151903]

Meredith MM, Liu K, Darrasse-Jeze G, Kamphorst AO, Schreiber HA, Guermonprez P, Idoyaga J, Cheong C, Yao KH, Niec RE, Nussenzweig MC. Expression of the zinc finger transcription factor zDC (Zbtb46, Btbd4) defines the classical dendritic cell lineage. The Journal of experimental medicine. 2012; 209:1153–1165. [PubMed: 22615130]

Miller JC, Brown BD, Shay T, Gautier EL, Jojic V, Cohain A, Pandey G, Leboeuf M, Elpek KG, Helft J, et al. Deciphering the transcriptional network of the dendritic cell lineage. Nature Immunology. 2012; 13:888–899. [PubMed: 22797772]

Mitchell GF, Miller JF. Cell to cell interaction in the immune response. II. The source of hemolysin-forming cells in irradiated mice given bone marrow and thymus or thoracic duct lymphocytes. The Journal of experimental medicine. 1968; 128:821–837. [PubMed: 5691986]

Miyake Y, Asano K, Kaise H, Uemura M, Nakayama M, Tanaka M. Critical role of macrophages in the marginal zone in the suppression of immune responses to apoptotic cell-associated antigens. J Clin Invest. 2007; 117:2268–2278. [PubMed: 17657313]

Nilsson A, Vesterlund L, Oldenborg PA. Macrophage expression of LRP1, a receptor for apoptotic cells and unopsonized erythrocytes, can be regulated by glucocorticoids. Biochem Biophys Res Commun. 2012; 417:1304–1309. [PubMed: 22234309]

Oldenborg PA. CD47: A Cell Surface Glycoprotein Which Regulates Multiple Functions of Hematopoietic Cells in Health and Disease. ISRN Hematol. 2013; 2013:614619. [PubMed: 23401787]

Oldenborg PA, Gresham HD, Lindberg FP. CD47-signal regulatory protein alpha (SIRPalpha) regulates Fcgamma and complement receptor-mediated phagocytosis. The Journal of experimental medicine. 2001; 193:855–862. [PubMed: 11283158]

Oldenborg PA, Zheleznyak A, Fang YF, Lagenaur CF, Gresham HD, Lindberg FP. Role of CD47 as a marker of self on red blood cells. Science. 2000; 288:2051–2054. [PubMed: 10856220]

Pereira JP, Kelly LM, Xu Y, Cyster JG. EBI2 mediates B cell segregation between the outer and centre follicle. Nature. 2009; 460:1122–1126. [PubMed: 19597478]

Saito Y, Iwamura H, Kaneko T, Ohnishi H, Murata Y, Okazawa H, Kanazawa Y, Sato-Hashimoto M, Kobayashi H, Oldenborg PA, et al. Regulation by SIRPalpha of dendritic cell homeostasis in lymphoid tissues. Blood. 2010; 116:3517–3525. [PubMed: 20682853]

Sancho D, Reis e Sousa C. Signaling by myeloid C-type lectin receptors in immunity and homeostasis. Annu Rev Immunol. 2012; 30:491–529. [PubMed: 22224766]

Schakel K, von Kietzell M, Hansel A, Ebling A, Schulze L, Haase M, Semmler C, Sarfati M, Barclay AN, Randolph GJ, et al. Human 6-sulfo LacNAc-expressing dendritic cells are principal producers

of early interleukin-12 and are controlled by erythrocytes. Immunity. 2006; 24:767–777. [PubMed: 16782032]

Scharffetter-Kochanek K, Lu H, Norman K, van Nood N, Munoz F, Grabbe S, McArthur M, Lorenzo I, Kaplan S, Ley K, et al. Spontaneous skin ulceration and defective T cell function in CD18 null mice. The Journal of experimental medicine. 1998; 188:119–131. [PubMed: 9653089]

Scott CL, Tfp ZM, Beckham KS, Douce G, Mowat AM. Signal regulatory protein alpha (SIRPalpha) regulates the homeostasis of CD103(+) CD11b(+) DCs in the intestinal lamina propria. Eur J Immunol. 2014; 44:3658–3668. [PubMed: 25236797]

Shinall SM, Gonzalez-Fernandez M, Noelle RJ, Waldschmidt TJ. Identification of murine germinal center B cell subsets defined by the expression of surface isotypes and differentiation antigens. Journal of immunology. 2000; 164:5729–5738.

Steinman RM, Pack M, Inaba K. Dendritic cells in the T-cell areas of lymphoid organs. Immunol Rev. 1997; 156:25–37. [PubMed: 9176697]

Stewart A, Urbaniak S, Turner M, Bessos H. The application of a new quantitative assay for the monitoring of integrin-associated protein CD47 on red blood cells during storage and comparison with the expression of CD47 and phosphatidylserine with flow cytometry. Transfusion. 2005; 45:1496–1503. [PubMed: 16131383]

Subramanian M, Hayes CD, Thome JJ, Thorp E, Matsushima GK, Herz J, Farber DL, Liu K, Lakshmana M, Tabas I. An AXL/LRP-1/RANBP9 complex mediates DC efferocytosis and antigen cross-presentation in vivo. J Clin Invest. 2014; 124:1296–1308. [PubMed: 24509082]

Subramanian S, Parthasarathy R, Sen S, Boder ET, Discher DE. Species- and cell type-specific interactions between CD47 and human SIRPalpha. Blood. 2006; 107:2548–2556. [PubMed: 16291597]

Takai T, Li M, Sylvestre D, Clynes R, Ravetch JV. FcR gamma chain deletion results in pleiotrophic effector cell defects. Cell. 1994; 76:519–529. [PubMed: 8313472]

Takenaka K, Prasolava TK, Wang JC, Mortin-Toth SM, Khalouei S, Gan OI, Dick JE, Danska JS. Polymorphism in Sirpa modulates engraftment of human hematopoietic stem cells. Nat Immunol. 2007; 8:1313–1323. [PubMed: 17982459]

Tsai RK, Discher DE. Inhibition of "self" engulfment through deactivation of myosin-II at the phagocytic synapse between human cells. J Cell Biol. 2008; 180:989–1003. [PubMed: 18332220]

Tseng D, Volkmer JP, Willingham SB, Contreras-Trujillo H, Fathman JW, Fernhoff NB, Seita J, Inlay MA, Weiskopf K, Miyanishi M, Weissman IL. Anti-CD47 antibody-mediated phagocytosis of cancer by macrophages primes an effective antitumor T-cell response. Proc Natl Acad Sci U S A. 2013; 110:11103–11108. [PubMed: 23690610]

Turner L, Ward SG, Westwick J. RANTES-activated human T lymphocytes. A role for phosphoinositide 3-kinase. Journal of immunology. 1995; 155:2437–2444.

Van VQ, Lesage S, Bouguermouh S, Gautier P, Rubio M, Levesque M, Nguyen S, Galibert L, Sarfati M. Expression of the self-marker CD47 on dendritic cells governs their trafficking to secondary lymphoid organs. EMBO Journal. 2006; 25:5560–5568. [PubMed: 17093498]

Wang H, Madariaga ML, Wang S, Van Rooijen N, Oldenborg PA, Yang YG. Lack of CD47 on nonhematopoietic cells induces split macrophage tolerance to CD47null cells. Proc Natl Acad Sci U S A. 2007; 104:13744–13749. [PubMed: 17699632]

Washio K, Kotani T, Saito Y, Respatika D, Murata Y, Kaneko Y, Okazawa H, Ohnishi H, Fukunaga A, Nishigori C, Matozaki T. Dendritic cell SIRPalpha regulates homeostasis of dendritic cells in lymphoid organs. Genes Cells. 2015; 20:451–463. [PubMed: 25818708]

Witmer MD, Steinman RM. The anatomy of peripheral lymphoid organs with emphasis on accessory cells: light-microscopic immunocytochemical studies of mouse spleen, lymph node, and Peyer's patch. American Journal of Anatomy. 1984; 170:465–481. [PubMed: 6475812]

Woolf E, Grigorova I, Sagiv A, Grabovsky V, Feigelson SW, Shulman Z, Hartmann T, Sixt M, Cyster JG, Alon R. Lymph node chemokines promote sustained T lymphocyte motility without triggering stable integrin adhesiveness in the absence of shear forces. Nat Immunol. 2007; 8:1076–1085. [PubMed: 17721537]

Yamamoto M, Sato S, Hemmi H, Hoshino K, Kaisho T, Sanjo H, Takeuchi O, Sugiyama M, Okabe M, Takeda K, Akira S. Role of adaptor TRIF in the MyD88-independent toll-like receptor signaling pathway. Science. 2003; 301:640–643. [PubMed: 12855817]

Yi T, Cyster JG. EBI2-mediated bridging channel positioning supports splenic dendritic cell homeostasis and particulate antigen capture. Elife. 2013; 2:e00757. [PubMed: 23682316]

Zimring JC, Hendrickson JE. The role of inflammation in alloimmunization to antigens on transfused red blood cells. Curr Opin Hematol. 2008; 15:631–635. [PubMed: 18832936]

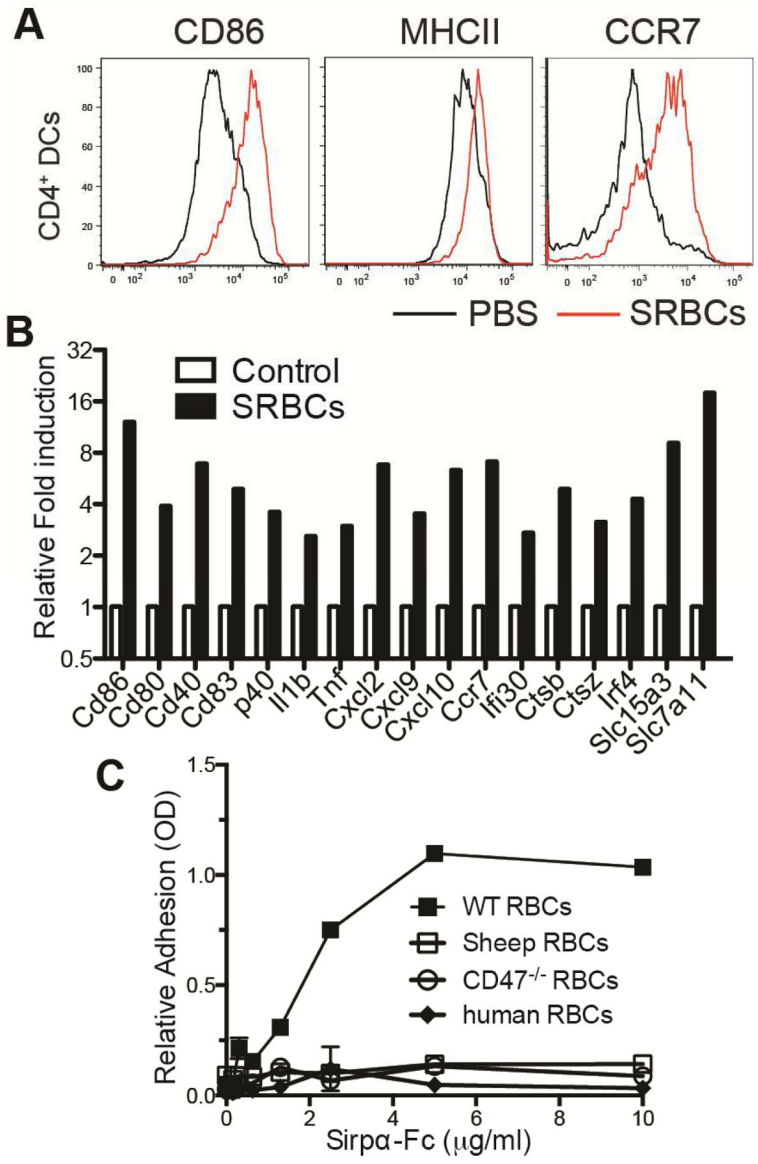

Figure 1. Xenogeneic RBCs activate splenicCD4$^+$ DCs

(A) Mice were i.v. immunized with SRBC or PBS control and analyzed 3 hr later by flow cytometry for CD86, MHCII, and CCR7 in gated CD4$^+$ DCs. One representative flow cytometry pattern is shown (n>6 animals). **(B)** Gene expression in CD4$^+$ DCs from mice immunized with SRBCs 1 hr earlier relative to CD4$^+$ DCs from PBS (control) treated mice, determined by RNAseq analysis. Average of two replicated experiments is shown. See also Table S1. **(C)** Binding of WT or *Cd47*$^{-/-}$ mouse, sheep, and human RBCs to plate-bounded Sirpα-Fc. The experiment was independently replicated three times with RBCs from different mice, sheep, and human donors. See also Figure S1.

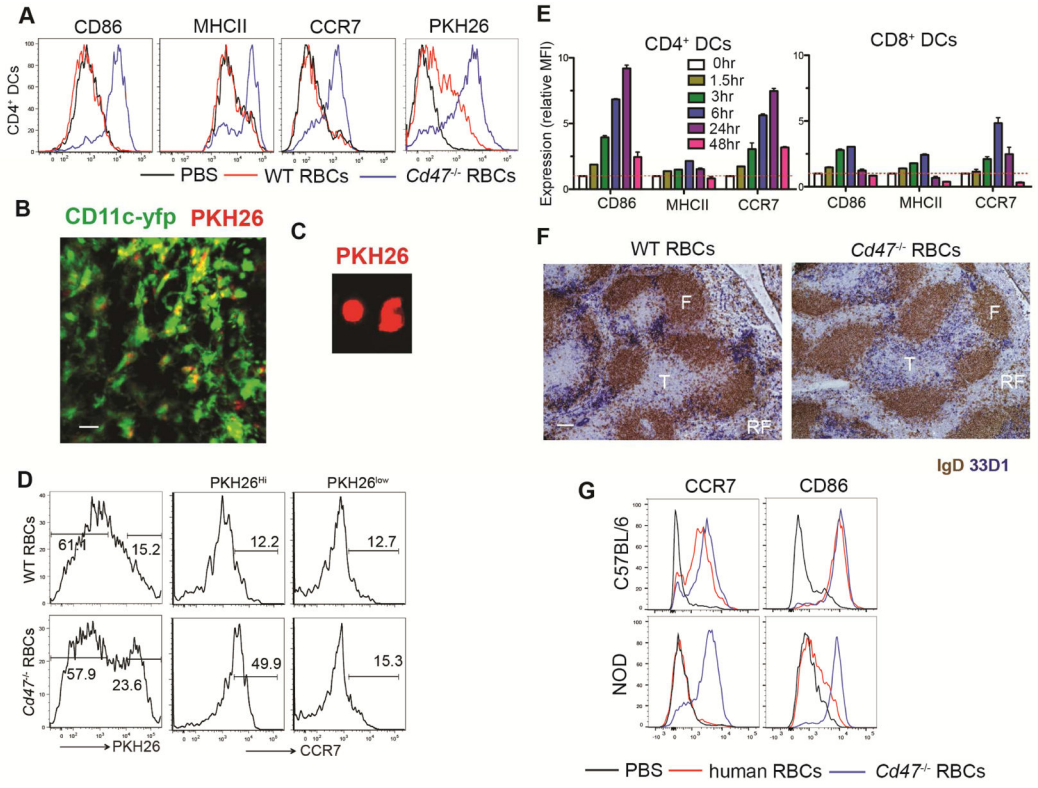

Figure 2. Activation and uptake of CD47-deficient RBCs by splenic CD4$^+$ DCs

(A) Mice were immunized with 30 μl PKH26-labeled RBCs from WT or *Cd47*$^{-/-}$ mice and analyzed 3 hr later by flow cytometry for CD86, MHCII, CCR7 and PKH26 in gated CD4$^+$ DCs. **(B)** CD11c-yfp mice were immunized with 30 μl PKH26-labeled RBCs from *Cd47*$^{-/-}$ mice. 20min after immunization, spleens were vibratome-sectioned and imaged using two-photon microscopy for YFP and PKH26. Scale bar, 20 μm. See also Movie S1. (C) Fluoresce microscopy detection of PKH26 in flow cytometry sorted CD11c$^+$MHCII$^+$CD4$^+$ DCs from WT mice immunized 30 min earlier with PKH26-labeled *Cd47*$^{-/-}$ RBCs. **(D)** Mice were i.v. immunized with 5μl PKH26-labeled WT or *Cd47*$^{-/-}$ RBCs and CD4$^+$ DCs were analyzed 3hr later by flow cytometry for PKH26 and for CCR7. CCR7 staining is shown for CD4$^+$ DCs gated on PKH26^{Hi} and PKH26^{low} cells as in plots on left. **(E)** Mice were immunized with 30 μl *Cd47*$^{-/-}$ RBCs and mean fluorescence intensity (MFI) of the indicated markers on gated CD4 or CD8$^+$ DCs relative to that of untreated mice was determined at the indicated time points (mean ± SE, n=3). **(F)** Mice were immunized with 30 μl WT or *Cd47*$^{-/-}$ RBCs and 6 hr later spleen sections were stained for DCIR2 (33D1, blue) and IgD (brown). F, follicle; T, T cell zone; RP, red pulp. Scale bar, 100 μm. **(G)** C57BL/6 or NOD mice were i.v. immunized with PBS, human RBCs, and *Cd47*$^{-/-}$ RBCs, and analyzed 6 hr later by flow cytometry for CCR7 and CD86 in gated CD4$^+$ DCs. All above experiments have been independently replicated with at least 3–5 animals. See also Figure S2.

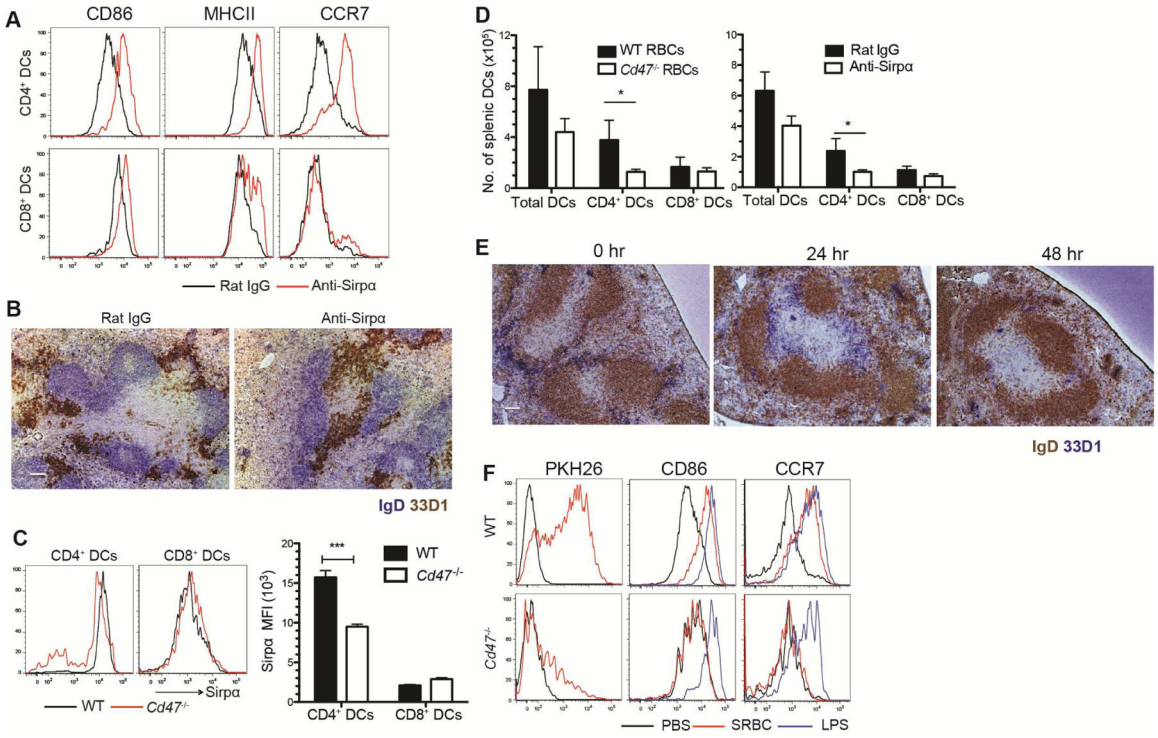

Figure 3. Blockade of Sirpa activates splenic CD4$^+$ DCs and leads to their loss

(A) Mice were i.v. injected with anti-Sirpα or control rat IgG2a and analyzed 6 hr later by flow cytometry for CD86, MHCII, and CCR7 in gated CD4 and CD8$^+$ DCs (n=3 mice) **(B)** Immunochemistry staining of IgD and DCIR2 (33D1) in splenic sections from mice treated as in A. Scale bar, 100 μm. **(C)** Flow cytometric analysis of Sirpα expression in gated CD4$^+$ and CD8$^+$ DCs from WT or *Cd47*$^{-/-}$ mice. Left panel, representative flow cytomtery pattern; right panel, mean fluorescence intensity (MFI) of Sirpα expression (mean ± SE, n=3 mice from two experiments). **(D)** Mice were i.v. injected with 30 μl *Cd47*$^{-/-}$ RBCs or anti-Sirpα and numbers of splenic DCs were quantified 3 days later by flow cytometry (mean ± SE, n=3 mice). **(E)** Mice were i.v. injected with *Cd47*$^{-/-}$ RBCs and spleen sections stained for IgD and DCIR2 (33D1) at the indicated time points. Scale bar, 100 μm. **(F)** WT or *Cd47*$^{-/-}$ mice were i.v. injected with PBS, 30 ul PKH26-labeled SRBCs, or 20 μg LPS and then analyzed 3hr later by flow cytometry for PKH26, CD86, and CCR7 in gated CD4$^+$ and CD8$^+$ DCs. One representative flow cytometry pattern is shown (n=6 mice from two experiments). See also Figure S3.

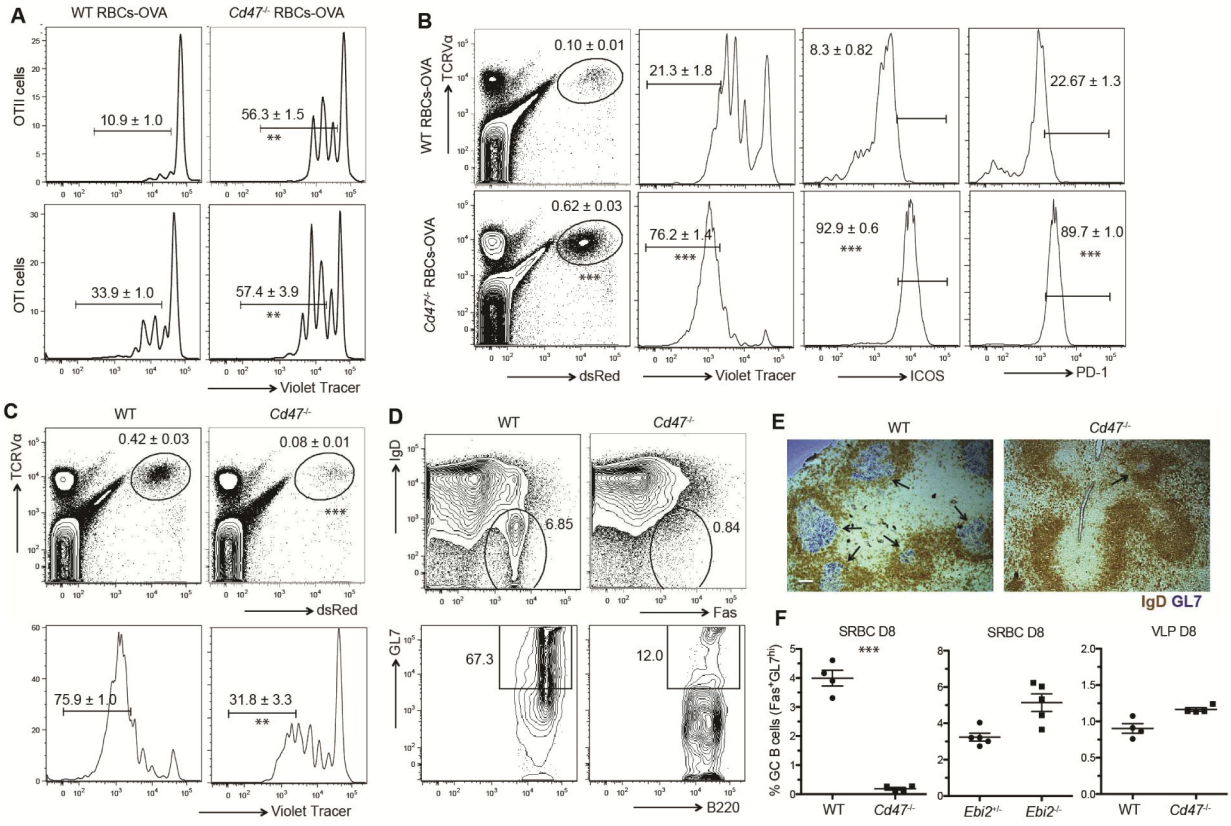

Figure 4. Adjuvant effect of CD47-deficient RBCs in CD4$^+$ T cell responses

(A, B) CD45.1$^+$ OTII or OTI splenocytes were labeled with cell trace violet, adoptively transferred to WT mice and 1 day later mice were immunized with WT or *Cd47*$^{-/-}$ RBC-OVA conjugate. **A**, Two days post-immunization, T cell proliferation was visualized by violet tracer dilution. **B**, Three days post-immunization, frequency of OVA specific OTII cells, violet tracer dilution, ICOS, and PD1 was examined by flow cytometry. Right three panels are gated on OTII T cells. Numbers on gates indicate mean (±SE) frequencies for three mice. **(C)** CD45.1$^+$ OTII splenocytes were labeled with cell trace violet, adoptively transferred to WT or *Cd47*$^{-/-}$ mice and 1 day later mice were immunized with SRBC-OVA conjugate. Frequency of OVA-specific OTII cells and violet tracer dilution on OTII cells was examined by flow cytometry 3 days post-immunization (mean ± SE, n=3 mice). (**D, E, F**) WT, *Cd47*$^{-/-}$ mice, *Ebi2*$^{+/-}$, and *Ebi2*$^{-/-}$ mice were immunized with SRBC or VLPs. Eight days after immunization, GC B cells were examined by flow cytometric analysis and immunochemistry staining. **D**, Representative flow cytometric pattern; **E**, representative spleen sections; GCs are marked with black arrows, and **F,** mean (±SE) frequency of IgD^{lo}Fas^{hi}GL7^{hi} GC B cells among total B cells in indicated mice. All experiments above were independently replicated at least two times with 3–5 mice each time. Scale bar in E, 100 μm. ** p<0.01, *** p<0.001 for unpaired student t test. See also Figure S4.

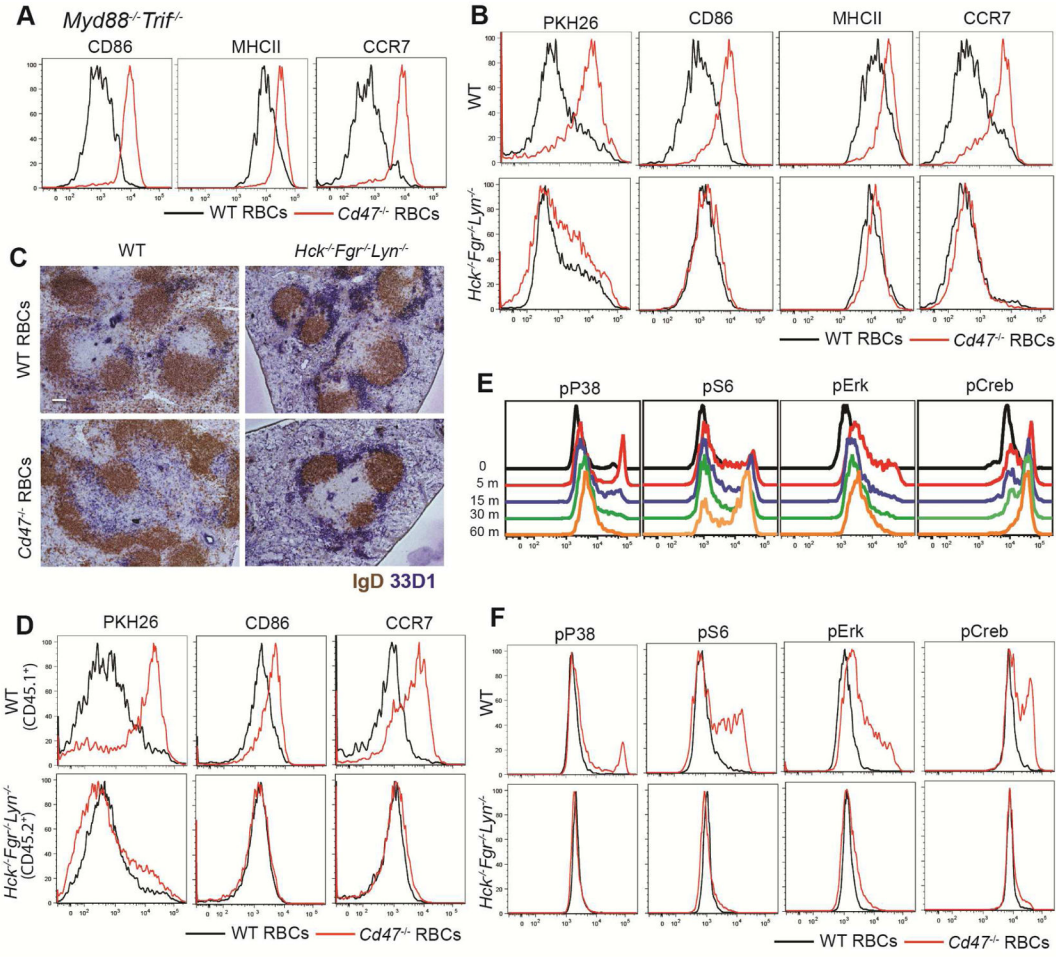

Figure 5. CD47-deficient RBCs activate Src family kinase signaling in CD4$^+$ DCs

(A) *Myd88*$^{-/-}$*Trif*$^{-/-}$ mice were immunized with WT or *Cd47*$^{-/-}$ RBCs and analyzed 3 hr later by flow cytometry for CD86, MHCII, and CCR7 in gated CD4$^+$ DCs (n=2 mice). **(B, C)** WT or *Hck*$^{-/-}$*Fgr*$^{-/-}$*Lyn*$^{-/-}$ mice were immunized with PKH26-labeled WT or *Cd47*$^{-/-}$ RBCs. **B**, flow cytometric analysis of PKH26, CD86, MHCII, and CCR7 in gated CD4 $^+$DCs 3 hrs after immunization (n=5 mice from 3 experiments). **C**, Immunohistochemical staining of DCIR2 (33D1) and IgD in spleen sections taken 6 hr after immunization. Scale bar, 100 μm. **(D)** Wild-type CD45.1$^+$ mice were lethally irradiated and reconstituted with mixed BM cells (1:1 ratio) from CD45.1$^+$ WT mice and CD45.2$^+$ *Hck*$^{-/-}$*Fgr*$^{-/-}$*Lyn*$^{-/-}$ mice. Chimeras were immunized with PKH26-labeled WT or *Cd47*$^{-/-}$ RBCs and analyzed 3 hr later by flow cytometry for PKH26, CD86, and CCR7 in gated CD4$^+$ DCs (n=4 mice in each group from two experiments). (**E**) WT mice were immunized with *Cd47*$^{-/-}$ RBCs and splenocytes were fixed at the indicated time points and phospho-p38, -S6, -Erk, and -Creb were examined in CD4$^+$ DCs by intracellular flow cytometric staining (n=3 mice). **(F)** WT or *Hck*$^{-/-}$*Fgr*$^{-/-}$*Lyn*$^{-/-}$ mice were immunized with WT or *Cd47*$^{-/-}$ RBCs for 5 minutes before staining as in E. One representative of three replicated experiments is shown. See also Figure S5.

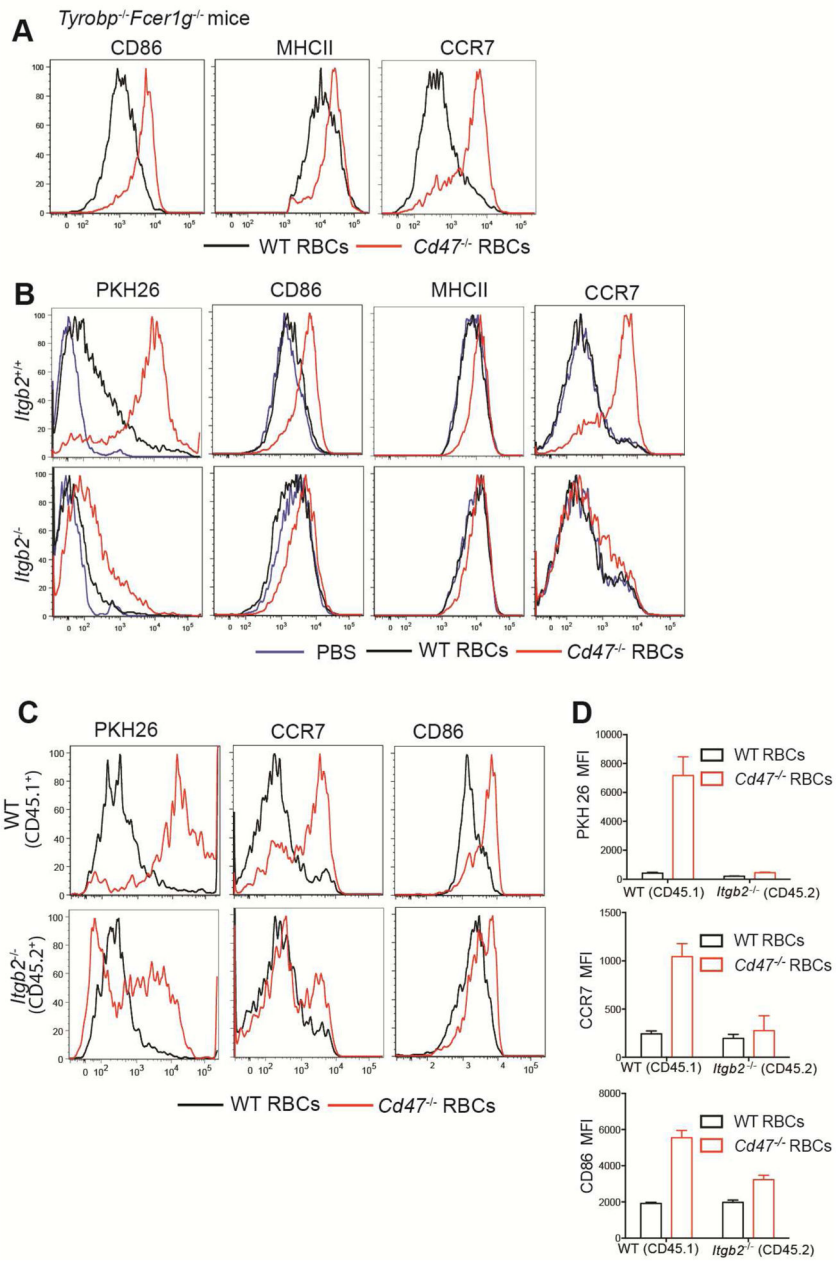

Figure 6. CD18-integrin involvement in RBC-mediated DC activation

(A) *Tyrobp*$^{-/-}$*Fcer1g*$^{-/-}$ mice were i.v. immunized with WT or *Cd47*$^{-/-}$ RBCs and analyzed 3hr later by flow cytometry for CD86, MHCII, and CCR7 in gated CD4^{+} DCs (n=4 mice from two experiments). **(B)** *Itgb2*$^{+/+}$ and *Itgb2*$^{-/-}$ BM chimeras were immunized with PBS, or PKH26-labeled WT or *Cd47*$^{-/-}$ RBCs. Flow cytometric analysis of PKH26, CD86, MHCII, and CCR7 in gated DCIR2 (33D1)$^{+}$ DCs 3 hrs after immunization is shown (n=5 mice in two experiments). **(C, D)** Wild-type CD45.1^{+} mice that had been reconstituted with a 1:1 mixture of BM cells from CD45.1^{+} WT and CD45.2^{+} *Itgb2*$^{-/-}$ mice were immunized with PKH26-labeled WT or *Cd47*$^{-/-}$ RBCs and analyzed 3 hr later. **C**, representative flow cytometry pattern for PKH26, CD86, and CCR7 in gated CD4^{+} DCs; **D**, mean (± SE) of

mean fluorescence intensity (MFI) for the indicated markers (n=3 mice). One representative of three replicated experiments is shown. See also Figure S6.